To appear in the Oct. 1, 2003 Astrophysical Journal
Preprint typeset using LaTeX style emulateapj v. 11/12/01

arXiv:astro-ph/0307121v1 7 Jul 2003

MAGNETIC WHITE DWARFS FROM THE SDSS. THE FIRST DATA RELEASE[1]

Gary D. Schmidt[2], Hugh C. Harris[3], James Liebert[2], Daniel J. Eisenstein[2], Scott F. Anderson[4], J. Brinkmann[5], Patrick B. Hall[6,7], Michael Harvanek[5], Suzanne Hawley[4], S. J. Kleinman[5], Gillian R. Knapp[6], Jurek Krzesinski[5,8], Don Q. Lamb[9], Dan Long[5], Jeffrey A. Munn[3], Eric H. Neilsen[10], Peter R. Newman[5], Atsuko Nitta[5], David J. Schlegel[6], Donald P. Schneider[11], Nicole M. Silvestri[4], J. Allyn Smith[12], Stephanie A. Snedden[5], Paula Szkody[4], and Dan Vanden Berk[13]
gschmidt@as.arizona.edu

To appear in the Oct. 1, 2003 Astrophysical Journal

ABSTRACT

Beyond its goals related to the extragalactic universe, the Sloan Digital Sky Survey (SDSS) is an effective tool for identifying stellar objects with unusual spectral energy distributions. Here we report on the 53 new magnetic white dwarfs discovered during the first two years of the survey, including 38 whose data are made public in the 1500 square-degree First Data Release. Discoveries span the magnitude range $16.3 \leq g \leq 20.5$, and based on the recovery rate for previously-known magnetic white dwarfs, the completeness of the SDSS appears to be high for reasonably hot stars with $B \gtrsim 3$ MG and $g \gtrsim 15$. The new objects nearly double the total number of known magnetic white dwarfs, and include examples with polar field strengths $B_p > 500$ MG as well as several with exotic atmospheric compositions. The improved sample statistics and uniformity indicate that the distribution of magnetic white dwarfs has a broad peak in the range $\sim 5 - 30$ MG and a tail extending to nearly 10^9 G. Degenerates with polar fields $B_p \gtrsim 50$ MG are consistent with being descendents of magnetic Ap/Bp main-sequence stars, but low- and moderate-field magnetic white dwarfs appear to imply another origin. Yet-undetected magnetic F-type stars with convective envelopes that destroy the ordered underlying field are attractive candidates.

Subject headings: white dwarfs — stars:magnetic fields

1. INTRODUCTION

Among the many products of the Sloan Digital Sky Survey (SDSS; York et al. 2000; Stoughton et al. 2002) will be thousands of new white dwarfs extending to fainter than 20th mag. and distances greater than 1 kpc. Local samples show that ∼10% of white dwarfs are magnetic in the range $10^4 - 10^9$ G (Kawka et al. 2003; Liebert, Bergeron & Holberg 2003; see also Schmidt & Smith 1995). Thus, when the SDSS is complete to at least 7,000 square degrees, the list of 60-odd previously-known magnetic white dwarfs (e.g., Wickramasinghe & Ferrario 2000) will be increased several times over. The new catalog will enable a number of statistical tests of roles that magnetic fields might play in stellar evolution, and will almost certainly display new atomic and molecular species in magnetic fields beyond what have been observed to date. A hint of what can be expected is provided by the 7 new magnetic white dwarfs identified by Gänsicke, Euchner, & Jordan (2002) in the first 462 square-degree Early Data Release (EDR). The current paper reports on the 60 magnetic white dwarfs identified thus far in the SDSS; 53 of which are new and 38 of which are contained in the First Data Release (DR1; Adelman et al. 2003) that covers the initial ∼1500 square degrees of the survey. Some of these stars have been reported in the preview by Harris et al. (2003).

2. OBSERVATIONS

The primary SDSS database is 5-color photometry (u, g, r, i, z) from which targets are selected for followup fiber spectroscopy with twin dual-beam spectrographs (3900 − 6200 Å and 5800 − 9200 Å). Both sets of data are obtained with the 2.5 m telescope at Apache Pt., New Mexico (see, e.g., Fukugita et al. 1996; Gunn et al. 1998; Lupton, Gunn, & Szalay 1999; York et al. 2000; Lupton et al. 2001). Astrometric data to an accuracy of ∼50 mas is also available (Pier et al. (2003), and provides important information for local stellar populations like white dwarfs. Target selection for the spectroscopic fibers is a somewhat involved process based on color criteria that have evolved slightly since the survey's inception. A brief summary can be found in Harris et al. (2003); more complete discussion will be deferred to a future publication. However, it is important to realize that only the coolest white dwarfs are targeted explicitly. Once the fiber data are reduced to flux-calibrated spectra, the objects are crudely classified. White dwarfs can be found in a number of categories, but because of their occasionally bizarre spectral characteristics, a search for magnetic white dwarfs must involve a variety of object categories, including QSOs and especially unclassifiable objects. Still, undoubtedly many white dwarfs do not receive a fiber, and the resulting incompleteness of the spectroscopic sample cannot be accurately assessed at this time. With a resolving power of ∼1800, SDSS spectroscopy is effective for recognizing magnetic splitting of the Balmer lines for $B > 1 - 3$ MG, depending on object brightness ($\Delta\lambda_Z \approx \pm 20$ Å MG^{-1} at Hα). The detection of weaker fields on white dwarfs requires high-resolution spectroscopy of the non-LTE line cores or a search for circular polarization in the line wings arising from the net longitudinal field component because the individual Zeeman lines are lost in the Stark-broadened profiles. Very strong magnetic fields can generally be recognized by the presence of broad, generally asymmetric absorption features at unusual wavelengths.

---

[1] A portion of the results presented here were obtained with the MMT Observatory, a facility operated jointly by The University of Arizona and the Smithsonian Institution.

[2] Steward Observatory, The University of Arizona, Tucson AZ 85721.

[3] U.S. Naval Observatory, P.O. Box 1149, Flagstaff, AZ 86002-1149.

[4] Department of Astronomy, University of Washington, Box 351580, Seattle, WA 98195-1580.

[5] Apache Point Observatory, PO Box 59, Sunspot, NM 88349-0059.

[6] Princeton University Observatory, Peyton Hall, Princeton, NJ 08544-1001.

[7] Departamento de Astronomía y Astrofísica, Facultad de Física, Pontificia Universidad Católica de Chile, Casilla 306, Santiago 22, Chile.

[8] Obserwatorium Astronomiczne na Suhorze, Akademia Pedagogicazna w Krakowie, ulica Podchorążych 2, PL-30-084 Kraków, Poland.

[9] Dept. of Astronomy and Astrophysics, University of Chicago, 5640 South Ellis Avenue, Chicago, IL 60637.

[10] Fermi National Accelerator Laboratory, P.O. Box 500, Batavia, IL 60510.

[11] Pennsylvania State University, Department of Physics and Astronomy, 525 Davey Lab., University Park, PA 16802.

[12] Mailstop D448, Los Alamos National Lab, Los Alamos, NM 87545.

[13] Department of Physics and Astronomy, University of Pittsburgh, 3941 O'Hara Street, Pittsburgh, PA 15260.

We also present here the initial results of followup optical spectroscopy and circular spectropolarimetry being carried out for the unusual, more interesting, and uncertain SDSS magnetic white dwarfs. For the latter category, a detection of circular polarization in the continuum serves to confirm the presence of a strong magnetic field, since it is produced by magnetic dichroism in the stellar atmosphere at a rate ∼0.01% MG^{-1} (Schmidt 1989), dependent also on temperature and field orientation. The spectropolarimetric data were obtained during the period 2002 Feb. − Dec. with the instrument SPOL (Schmidt, Stockman, & Smith 1992) attached to the Steward Observatory 2.3 m Bok telescope on Kitt Peak and the 6.5 m MMT atop Mt. Hopkins. Data reduction was carried out as described by Schmidt et al. (1992).

3. RESULTS

Magnetic white dwarfs selected to date from the SDSS are summarized in Tables 1 − 3 for various spectral types. In each table, column (1) lists the SDSS identification in epoch 2000 coordinates, col. (2) the plate-MJD-fiber identifier for the SDSS spectrum, and cols. (3) and (4) the UT date and time of the spectroscopy. Spectroscopic exposure times are typically ∼45 min in length and are selected to achieve approximately uniform signal-to-noise ratio for a specified object brightness. Occasionally this requires multiple exposures over successive nights, so rotational smearing of the field patterns may be present, depending on the (unknown) spin period and details of the observation.

Polar field strengths and approximate viewing perspectives have been estimated where possible by comparing the SDSS data against model spectra for assumed inclined dipolar field patterns, and these results are listed in cols. (6) and (7). The modeling procedure is an outgrowth of the code developed by Latter, Schmidt, & Green (1987), using transition wavelengths and oscillator strengths from Kemic (1974) for $B_p \lesssim 30$ MG and the calculations summarized by Ruder et al. (1994) for higher fields. The procedure accounts for the change in line strength with field as well as the variation in B over the stellar surface, but does not solve for the temperature structure nor account for the transfer of polarized radiation through the atmosphere. This "geometric" approach is therefore adequate for estimating the effective polar field strength and orientation for a simple assumed field pattern like a centered or offset dipole, but not for evaluating the appropriateness of that geometry vs. more elaborate multipolar expansions from detailed spectropolarimetric data. An estimate of the reliability of the approach as compared with more elaborate procedures can be gained by a comparison of our results against those of Gänsicke et al. (2002) for the stars in the EDR. Overall, we regard the results quoted below to be accurate to better than 10% in B_p and ∼±30° in inclination for the field patterns assumed. That said, we note that the profiles of geometry-sensitive lines like the σ components of Hα are often not well modeled by a dipolar field pattern at *any* assumed inclination; we take this to indicate that the field patterns cannot be adequately described by simple centered dipoles. The final column of the tables provides aliases for previously-known objects and other comments, including the estimates of B_p and i by Gänsicke et al. for stars in common.

About 75% of all white dwarfs are type DA, and the 49 stars with hydrogen features in Table 1 also dominate the 60 magnetic candidates identified thus far in the SDSS. Field strengths of the stars span the range 1.5 MG to more than 500 MG, nearly as wide an interval as is covered by all previously-discovered magnetic white dwarfs. Caution must be exercised when evaluating the number distribution as a function of field strength, however, because of the aforementioned incompleteness at weak fields, and because the existence of a correlation between magnetism and remnant mass (e.g., Liebert 1988; Sion et al. 1988) implies that selection effects may be important in a magnitude-limited survey like the SDSS. Such biases should be carefully assessed when estimating relative space densities (Liebert et al. 2002). We return to this question in §6.2.

A selection of white dwarfs from Table 1 showing the hydrogen spectrum in low to moderate fields is shown in Figure 1. In the regime $0 < B \lesssim 50$ MG, Hα retains a triplet structure with ever-increasing separation but with the triplet components broadening as the l-degeneracy of the atom is removed. For considerably stronger fields, the magnetic effect can no longer be considered a perturbation and diagnosis is best done by searching for features at the locations of turnarounds or stationary points in the $B - \lambda$ curves. Examples of such stars with field strengths between 100 MG and 500 MG are compared to the principal features expected in Figure 2.

Only 4 magnetic DB stars were known prior to the SDSS: LB8827 has $B \lesssim 1$ MG and HE1211−1707, HE1043−0502, and GD 229 are all above 50 MG. Additionally, G227-28 and Feige 7 are magnetic stars with mixed H/He composition. Three new magnetic DB white dwarfs with $B < 10$ MG have been found in the SDSS and are displayed in Figure 3. Such stars are most easily recognized by the Zeeman triplet at He I λ5876, which is isolated and not easily confused with other features. These spectra have also been modeled for dipolar field strength and inclination using synthetic spectra based on the calculations of Kemic (1974), with the results listed in Table 2.

Two magnetic/nonmagnetic white dwarf pairs have been found in the SDSS that augment the 3 binaries known previously. Both magnetic stars are DAH spectral type and entered in Table 1, but as depicted in Figure 4, they are teamed with a nonmagnetic DA and DB. Such systems are potentially very interesting from evolutionary points of view, and the new examples are described individually below.

Finally, Table 3 collects stars that show absorption lines or bands of metals in magnetic fields, magnetic stars whose atmospheric species are as yet unknown, and objects that can only be classified as candidate magnetic white dwarfs at this time. These include the first DQ showing Zeeman-split C I lines and a magnetic DZ similar to LHS 2534 (Reid, Liebert, & Schmidt 2001). The spectra are displayed in Figures $5-6$ and discussed in more detail below. Note that field strengths for these stars, where available, are quoted as mean surface fields, B_s, since atomic data are generally insufficient to allow detailed modeling.

4. PHOTOMETRY AND STELLAR TEMPERATURES

The SDSS spectroscopy is known to occasionally display flux calibration irregularities due to variable fiber placement, atmospheric dispersion, and other effects. When present, these tend to be most prominent shortward of 4500 Å, so the observed spectral flux distribution is often not ideal for temperature estimation. A more accurate approach – the fitting of Balmer line profiles for simultaneous temperature and gravity determination – has been applied only rarely to magnetic white dwarfs (e.g., Schmidt et al. 1992) due to the uncertainties of line broadening, and a general approach has not yet been developed.

We have therefore gathered the "PSF photometry" from the imaging observations, using the beta version of the First Data Release (Adelman et al. 2003), specifically from version v5_3 of the `photo` pipeline. Note that this can be slightly different from the photometry upon which spectroscopic target decisions were made. The PSF photometry has systematic effects that are $\lesssim$2% for g through z and only slightly poorer in u (Hogg et al. 2001; Smith et al., 2002; Stoughton et al. 2002). The values are presented in Table 4.

Temperatures have been estimated for the magnetic stars by comparing their locations in the $u-g$ *vs.* $g-r$ plane against DA and DB colors computed for nonmagnetic stars from the models of Bergeron, Wesemael, & Beauchamp (1995; see also Harris et al. 2003). These results are also provided in Table 4. A few possible systematic effects should be noted. First, the equivalent widths of magnetically-split absorption lines generally increase with increasing field strength, and the patterns for the Balmer series begin to overlap for $\lambda \lesssim 4200$ Å at $B \sim 10$ MG. This can result in a depressed u magnitude and an erroneously cool temperature. Second, the magnitudes quoted are observed SDSS values; transformation coefficients for placing the photometry onto the AB system are not yet finalized and no reddening corrections have been made. Both corrections would be in the direction of making the colors bluer, with an effect on stellar temperatures of as much as 10%. A larger systematic difference exists between the temperatures quoted here compared with the continuum-based values of Gänsicke et al. (2002) for the same EDR magnetic white dwarfs; the latter are almost certainly overestimates since the pipeline processing of SDSS spectroscopy includes a reddening correction for an entire intervening Galactic disk. Finally, several entries in Table 4 are annotated by a colon (:) to denote unusually large uncertainties. These indicate the few cases where the stellar colors fall outside the loci for typical white dwarf gravities, as well as those examples with fields $\gtrsim 100$ MG, where continuum opacities depart substantially from the zero-field forms (and are unknown). Of course, temperatures for the two composite-spectrum objects represent the overall flux distribution, and DA atmospheres were assumed in both cases.

5. NOTES ON INDIVIDUAL OBJECTS

SDSS J0042+0019 and SDSS J0847+4842: Both of these stars are almost certainly magnetic+nonmagnetic double-degenerate binaries. SDSS J0042+0019[14] (Figure 4) displays Zeeman-split Balmer lines suggesting a field of $B_p \approx 14$ MG, but the π components are too strong compared with the σ lines for any reasonable field pattern. We interpret the spectrum as a composite DA+DAH with little radial velocity difference between the stellar components at the time of observation. SDSS J0847+4842 exhibits very broad lines of hydrogen plus narrower, undisplaced features of He I. Our followup spectropolarimetry, shown in the same figure, supports the DAH+DB classification, with strong $\mathcal{S}$-wave circular polarization signatures across Hβ and Hγ but no polarization reversals in the helium lines. Without resolving the Balmer line cores, it is difficult to estimate the surface field strength on the magnetic star; the magnitude of the longitudinal Zeeman effect in polarization suggests a field of a few MG. This inability to resolve the Balmer lines cores may also indicate a high rotation velocity on the magnetic component, such as would result from accretion. Further observations are warranted to determine the periods of these binaries.

SDSS J0157+0033: This is only the second magnetic DZ star known, showing lines of Mg I, Na I, and Ca I. As discussed by Reid et al. (2001) for LHS 2534 (which is recovered here as SDSS J1214−0234 and compared with SDSS J0157+0033 in Figure 5), the relative importance of magnetic and spin-orbit effects varies among these features for a field strength of a few MG. The Na I D lines, with a fine-structure splitting of 6 Å, decouple first, near a field of 1 MG. Thus, a deep triplet centered at λ5893 in LHS 2534 was interpreted in terms of the linear Zeeman effect and provided an estimate for the mean field of $B_s = 1.92$ MG. At that field strength, the magnetic and spin-orbit effects are comparable for the Mg I b lines, and four rather evenly-spaced components were observed, displaced somewhat to the red of the zero-field triplet.

---

[14] For brevity, we refer to Sloan targets as SDSS J*hhmm*±*ddmm* in the text of this paper.

Like LHS 2534, the spectrum of SDSS J0157+0033 shows a feature at 5893 Å which we take to be the π component of Na I D in an ordinary magnetic triplet. A second line at 5834 Å can then be interpreted as the σ^- component, implying $B_s = 3.7$ MG. The predicted location of the σ^+ component is indicated in Figure 5, but noise in the spectrum prevents a clear identification. The stronger field on SDSS J0157+0033 as compared with LHS 2534 suggests that the Mg I lines may have also entered the Paschen-Back regime, where a linear interpretation is adequate. Indeed, a simple model for $B = 3.7$ MG reveals that the nine components have arranged themselves by overlap into three distinct features, with wavelengths of ∼5128, 5176, and 5221 Å. The match of these against features in the observed spectrum is also indicated in Figure 5, confirming the field strength determination from the sodium lines. Ca I λ4226 is also present in absorption, but any magnetic splitting is contained within the broadened profile. Finally, several sharp features around 8500 Å deserve mention. While some of these might be interpreted as Zeeman components of Ca II $\lambda\lambda 8498 - 8662$, most are artifacts of the data (cf. the spectrum of SDSS J1036+6522 directly above in Figure 5). The behavior of the Ca II H and K lines has been studied in the appropriate field strength regime (Kemic 1975), but we are not aware of any computations of the infrared triplet. Unfortunately, LHS 2534 provides no guidance, as the available spectra do not extend sufficiently far to the red.

We note that the spectrum of SDSS J0157+0033 is strongly blanketed below 5000 Å as indicated by both the spectroscopy and photometric colors. The effect is not as dramatic as for LHS 2534, suggesting a somewhat warmer temperature than that star's ∼6000 K. The lack of Hα in either star (a dip of dubious significance in SDSS J0157+0033 is centered 23 Å to the blue of Hα at zero field – too far to be the quadratic shift at 3.7 MG and too near to be the σ^- component) indicates that the atmospheres are primarily helium, but proper modeling should be carried out to verify this conclusion.

SDSS J0211+0031 and SDSS J2151+0031: Spectral features for each of these stars are weak, owing in part to the rather low surface temperatures. However, both are confirmed as magnetic from our followup circular polarimetry: $v = -2\% \pm 0.5\%$ for SDSS J0211+0038 and $-0.6\% \pm 0.2\%$ for SDSS J2151+0031, summed over the range $\lambda\lambda 4200 - 8200$. The field strength determinations of 490 MG and ∼300 MG, respectively, are based largely on the presence of a narrow feature near 5850 Å that we associate with a leisurely turnaround of the 2s0−3p0 component of Hα (Figure 2). For SDSS J0211+0038, this identification is confirmed by several other lines, however the λ5850 line is extremely weak in SDSS J2151+0031 and our field strength estimate must be considered tentative pending better quality spectra.

SDSS J0333+0007 and SDSS J0005−1002: Discovered by Reimers et al. (1998) as HE0330−0002 and proven to be magnetic by Schmidt et al. (2001), this star was recovered in the EDR (Gänsicke et al. 2002). The white dwarf probably has a He-dominated atmosphere but the absorption features, seen in Figure 5, have not been successfully ascribed to He I. Indeed, comparison of the $u - g$ and $g - r$ colors (+0.47 and +0.13, respectively) to pure helium atmospheric models suggests a temperature of 7500 K, too cool to produce helium transitions. Any of a variety of trace species such as carbon and/or carbon-based molecules are possible. The candidate magnetic star SDSS J0005−1002 shows two strong troughs between 4000 − 4500 Å as well as weak, diffuse features around 5000 Å, near the position of Hα, and possibly at ∼7150 Å. Several of these approximate the locations of C I and C II lines seen in relatively hot DQ stars (Liebert 1977; Harris et al. 2003). The dip around 6580 Å even shows a hint of triplet structure suggesting a mean magnetic field of ∼3 MG. However, several of the features are weak and lines in the blue may be affected by flux calibration problems, so further spectroscopy and polarimetry are required to clarify the nature of this star.

SDSS J0933+0051, SDSS J1113+0146, and SDSS J1333+0016: The latter two stars are nearly spectroscopic twins to LP 790-29 and LHS 2229, respectively (Liebert et al. 1978; Schmidt et al. 1999). Spectropolarimetry shown in the same figure demonstrates that, like LP 790-29 and LHS 2229, both are strongly magnetic, with stronger polarization seen in the bands. The extremely deep, overlapping features (Figure 6) are generally reminiscent of the C_2 Swan bands, and Bues (1999) has shown that LP 790-29 can be modeled using these features in a magnetic field of ∼50 MG. The additional wavelength shift of ∼100 Å to the blue for SDSS J1113+0146 suggests that its field may be somewhat higher. For LHS 2229 and SDSS J1333+0016, the band progression is certainly molecular in origin, but the appearance is more scalloped and the species responsible is not yet determined. One possibility is C_2H (Schmidt et al. 1999). SDSS J0933+0051 appears to show the same structure, but the bands are far weaker. These stars are also discussed by Harris et al. (2003).

SDSS J1036+6522: The key clues to a magnetic interpretation of SDSS J1036+6522 are the triplets centered at 4772, 5382, and ∼7122 Å. In order, these match wavelengths of C I transitions: $3s\,^3P^0 - 4p\,^3P$, $3s\,^1P^0 - 4p\,^1P$, and a blend of $3p\,^3D - 4d\,^3F^0$ and $3p\,^3D - 5s\,^3P^0$. The splitting of ±31, 39, and 68 Å, respectively, implies a mean field strength $B_s = 2.9$ MG, suggesting a polar field strength for an assumed dipolar pattern of ∼4 MG. Another depression centered near 5050 Å is primarily C I $3s\,^1P^0 - 4p\,^1D$, and additional weaker features are probably present. SDSS J1036+6522 is the first DQ star that clearly shows magnetically-split lines of atomic carbon, and thus is an interesting example of a new magnetic species. White dwarfs of spectral type DQ – those with atomic features as well as the C_2 variety – are generally thought to have helium-rich atmospheres enriched by convective dredge-up from the carbon core (e.g., Liebert 1983; Pelletier et al. 1986).

SDSS J2247+1456: This star is the highest-field example found thus far in the SDSS and one of the brightest at $r = 17.6$. In total flux, the widely displaced Balmer components are reminiscent of those in the most strongly magnetic white dwarf known, PG 1031+234 (Schmidt et al. 1986). Followup spectropolarimetry obtained at the MMT is shown in Figure 7. Here we see that in circular polarization SDSS J2247+1456 also closely resembles PG 1031+234, with values reaching nearly −10% in the blue and a large amount of structure in the lines.

Faraday effects are clearly important in the atmosphere, as all features show positive intrinsic circular polarization regardless of whether they represent σ^+ components (e.g., most of the lines shortward of 5000 Å and the pair around 7000 Å) or π components (the sharp line due to the turnaround of $2s0 - 3p0$ near 5850 Å; cf. Figure 2). Such effects are expected (e.g., Achilleos & Wickramasinghe 1995; Wickramasinghe & Ferrario 2000) and are also seen in PG 1031+234. However, adequate modeling of high-field situations has not yet been carried out, despite the fact that such efforts might well lead to a better understanding of continuous opacity sources in highly magnetized atmospheres.

SDSS J2322+0039: Our solution for this star, B_p = 19 MG, $i \sim 60°$, is significantly different from the low-inclination, 13 MG determination of Gänsicke. This is the only such discrepancy for the magnetic DA stars in common between the analyses. However, we note that the discrimination between low-field/low-inclination and higher-field/high-inclination options can be somewhat problematic with spectra of limited quality, as the two solutions yield similar mean surface ("effective") field strengths.

SDSS J2323−0046: Gänsicke et al. (2002) interpret the broad depressions near Hβ and Hγ (Figure 3) as Zeeman-smeared features of hydrogen in a field of ∼30 MG, but point out the existence of narrower lines that may be due to He I. Close inspection reveals that He I λ5876 is actually a Zeeman triplet indicating a field $B_p \sim 5$ MG, and λ6678 is consistent with the same interpretation. Lacking evidence of Hα, we interpret the broad features in the blue as confluences of He I lines, some of which are indicated in Figure 3. As implied by Gänsicke et al., it is conceivable that this star is a DA+DBH binary, and further spectroscopy and spectropolarimetry should be carried out to evaluate this possibility.

6. DISCUSSION

6.1. *Distribution with Temperature*

The lifetime of a low-order magnetic field against free ohmic decay has been computed to be more than 10^9 yr (e.g., Chanmugam & Gabriel 1972; Muslimov, Van Horn, & Wood 1995), and observational support for this result can be found in the lack of a dependence of field strength on stellar temperature (e.g., Wickramasinghe & Ferrario 2000). With temperature estimates for the new SDSS examples covering the range ∼7000 K − 30,000 K, this lack of correlation is emphatically verified, both when the new stars are analyzed alone and when taken as part of the entire 116-object magnetic sample. It would appear that the magnetic fields on white dwarfs indeed behave like amplified, fossil remnants from earlier stages of evolution.

6.2. *Distribution with Field Strength*

The improved statistics provided by the SDSS discoveries warrant a new look at the distribution of magnetic white dwarfs as a function of field strength. In Figure 8 we present this as a histogram *vs.* polar field strength for both the SDSS discoveries (solid) and for all 116 examples known at the present time (hatched). Bins represent equal intervals in $\log B_p$, and polar field strengths are taken from spectral models where available. For stars that have not yet been successfully interpreted, field strengths are estimated from the degree of continuum circular polarization. Such estimates are particularly crude, but we do not wish to bias the results by omission, and the number of unsolved stars is sufficiently small that an error of a factor 2 or so in field strength will not affect the interpretation.

When evaluating the field strength distribution, the relative completeness of search techniques must be questioned. Because the discovery of magnetic fields below ∼2 MG requires the rather specialized techniques of spectropolarimetry, high-resolution spectroscopy of Balmer-line cores, or asteroseismology, lists are incomplete here. Thus, we focus attention on field strengths $B_p > 3$ MG, where the SDSS has already doubled the number of known magnetic stars. The discovery of white dwarfs of any type by spectroscopic classification from the SDSS depends in large part on the complicated algorithm the project uses for selecting the subset of detected sources for spectroscopy. An important consideration is that point sources with unusual colors often receive fibers because one of the SDSS categories is "serendipity" (see below). Highly magnetic white dwarfs with broad, displaced, and distorted absorption lines may show quite unusual colors (e.g., SDSS J2247+1456 or esp. SDSS J1113+0146 and SDSS J1333+0016!) and so be targeted for spectroscopic followup. This is particularly true for $T \lesssim 9,000$ K, where the colors of low-to-moderate field magnetic white dwarfs approach the locus of metal-poor main sequence stars, but magnetic degenerates with strong absorption features may remain outside of the stellar locus. For hotter white dwarfs, the magnetic white dwarfs with fields below 100 MG or so probably have a similar selection probability as nonmagnetic stars.

Such considerations suggest that the histogram of field strengths plotted in Figure 8 may actually be biased in favor of the highest fields. This makes the apparent peak around 5 MG − 30 MG all the more compelling. The currently popular scenario for the origin of magnetic white dwarfs is that they evolve from magnetic Ap and Bp stars. Such stars are found to occupy the range 2.8 kG $< \langle B \rangle <$ 30 kG, and the low-field cutoff is claimed to be *not* the result of selection effects (Mathys 2001). If we assume a factor of 10^4 for the typical amplification factor due to flux-freezing during formation of the degenerate core, and that a factor of 2 is reasonable for the scaling between the mean surface field and the polar field strength of the equivalent dipole, we find that the Ap/Bp hypothesis is most applicable for the highest-field magnetic white dwarfs, with ∼50 MG $\lesssim B_p \lesssim$ 500 MG. Another origin would seem to be required for the magnetic degenerates with weaker fields. Because of their comparatively large number, yet-undetected magnetic F main sequence stars would appear to be attractive candidates.

6.3. *Completeness of the SDSS for Magnetic White Dwarfs*

Some idea of the effectiveness of the fiber assignment and inspection process for identifying magnetic white dwarfs can be gained by comparing samples of objects found by different techniques. First, we have concurred with all of the magnetic identifications of Gänsicke et al. (2002), and we have added 2 magnetic stars that were not noted by them but were included in the EDR: SDSS J1729+5632 is a DA star displaying a moderate field but its spectrum is of relatively low signal-to-noise ratio, and SDSS J0211+0031 is a high-field DA with weak, highly-displaced features.

Of greater significance is the recovery rate for known magnetic white dwarfs whose positions have been included in the survey. Eight such stars are located in regions covered by the imaging survey of DR1: KUV03292+0035, HE0330−0002, G111-49, PG1015+015, GD90, G195-19, LBQS1136−0132, and Feige 7. Additionally, LHS 2534 and G99-37 were surveyed but are outside DR1 and LHS 2534 received a fiber. Six of the previously-known magnetic stars received fibers and were visually recognized as magnetic by team members who were blind to the identities of the stars. Of the remainder, Feige 7, G195-19, and G99-37 exceed the brightness threshold for detector saturation during a typical spectroscopic exposure and so cannot be fiber candidates (Stoughton 2002). The net result – 5 of the 6 qualifying magnetic white dwarfs within DR1 were recovered – suggests that the overall success rate is high for identifying targets fainter than about magnitude 15 and with temperatures similar to those that dominate existing white dwarf catalogs. As might be expected, both previously-known objects with very odd spectra were recovered: the unexplained HE0330−0002 and the strong-line magnetic DZ LHS 2534 (Figure 5).

The current level of completeness and its prognosis for future releases of the survey can also be assessed by inquiring into the fiber selection criteria used for the SDSS magnetic white dwarfs. Referring to the distribution among SDSS target selection categories (e.g., Stoughton et al. 2002), 22 of the 60 stars fell into the QSO region of color space, and an additional 13 stars were chosen as HOT_STD (hot subdwarf standard). Thus, nearly 60% of the magnetic white dwarfs appeared in high-priority categories for which spectroscopic fibers are nearly assured. The remaining targets fell off the stellar locus in categories SERENDIPITY_BLUE (14 stars), SERENDIPITY_DISTANT (7), or were correctly picked out as hot white dwarfs in STAR_WHITE_DWARF (4 stars). These three classes receive rather low priority for spectroscopy, and the resulting sky coverage is highly nonuniform. However, if we assume that a) 60% of magnetic white dwarfs will always appear in the spectroscopic database, b) the remaining 40% have possibly a 50:50 chance of being targeted, and c) that manual inspection is very efficient at recognizing magnetic spectra, we can broadly account for the high fraction of recovered magnetic stars. Of course, future results will be subject to changes in the procedures, including any refinement of the color criteria for the various object categories.

Finally, photometry and astrometric information is available for the imaged, but unrecovered, magnetic stars. For completeness this information is included as Table 5. Note that G195-19 in particular is so bright that the *gri* magnitudes are uncertain.

7. SUMMARY AND CONCLUSIONS

Despite the fact that the SDSS is tailored to extragalactic criteria, the survey is proving to be a rich source of unusual stellar objects. With roughly one quarter of the eventual sky coverage now completed, the known list of magnetic white dwarfs has nearly doubled in size, and new discoveries include the first low-field DB stars as well as magnetic examples of exotic atmospheric compositions like atomic and molecular carbon and metallic-line white dwarfs. Due to our very limited knowledge of the magnetic behavior of atomic and molecular species, a few high-field objects continue to frustrate efforts for line identification.

The list of magnetic+nonmagnetic white dwarf binaries that was previously comprised of LB11146 (Liebert et al. 1993), G62-46 (Bergeron, Ruiz, & Leggett 1993), and RX J0317−855 (=EUV0317−855; e.g., Barstow et al. 1995; Vennes et al. 2003) has grown by two. Both SDSS J0042+0019 and SDSS J0847+4842 deserve followup study to determine their periods and component masses. No double-magnetic systems have yet been found, and no detached magnetic white dwarf+main-sequence systems have been identified. The evolutionary implications of these results are not yet clear, but the rapid spin rate, high temperature, and extraordinarily large mass of RX J0317−855 suggest that magnetic fields may be acquired during the course of stellar evolution, at least when mergers are involved.

The efficiency of the overall identification pipeline for magnetic white dwarfs is high for reasonably hot stars with $B \gtrsim 3$ MG and $g \gtrsim 15$. The improved statistics and more uniform selection process provided by the SDSS has yielded a distribution of magnetic white dwarfs that peaks in the range ∼5 MG − 30 MG and shows a tail to several hundred MG. While it is reasonable to assume that the highest-field magnetic white dwarfs evolve from main-sequence Ap/Bp stars, the bulk of magnetic degenerates in this peak and below would appear to require an alternate source. Yet undetected magnetic F stars, whose convective envelopes would destroy an ordered underlying field structure with $B \sim 1$ G − 3 kG, would seem to be likely candidates.

Funding for the Sloan Digital Sky Survey has been provided by the Alfred P. Sloan Foundation, the Participating Institutions, the National Aeronautics and Space Administration, the National Science Foundation, the U.S. Department of Energy, the Japanese Monbukagakusho, and the Max Planck Society. The SDSS is a joint project of The University of Chicago, Fermilab, the Institute for Advanced Study, the Japan Participation Group, The Johns Hopkins University, Los Alamos National Laboratory, the Max-Planck-Institute for Astronomy (MPIA), the Max-Planck-Institute for Astrophysics (MPA), New Mexico State University, University of Pittsburgh, Princeton University, the United States Naval Observatory, and the University of Washington. We are grateful to the Directors of the Steward and MMT Observatories for awarding the observing time to follow up these discoveries, to M. Strauss for noting some of the magnetic candidates, and to P. Smith for assistance with the observations. Special thanks go to D.T. Wickramasinghe for general discussions about highly magnetic stars. Support was provided by NSF grant 97-30792.

REFERENCES

Achilleos, N., & Wickramasinghe, D.T. 1995, MNRAS, 272, 24

Adelman, J.A., et al. 2003, in preparation

Barstow, M.A., Jordan, S., O'Donoghue, D., Burleigh, M.R., Napiwotzki, R., & Harrop-Allin, M.K. 1995, MNRAS, 277, 971

Bergeron, P., Ruiz, M.-T., & Leggett, S.K. 1993, ApJ, 407, 733

Bergeron, P., Wesemael, F., & Beauchamp, A. 1995, PASP, 107, 1047

Bues, I. 1999, in ASP Conf. Ser. 169, Eleventh European Workshop on White Dwarfs, ed. J.E. Solheim & E.G. Meistas (San Francisco: ASP), 240

Chanmugam, G., & Gabriel, A.H. 1972, A&A, 16, 149

Fukugita, M., Ichikawa, T., Gunn, J.E., Doi, M., Shimasaku, K., & Schneider, D.P. 1996, AJ, 111, 1748

Gänsicke, B.T., Euchner, F., & Jordan S. 2002, A&A, 394, 957

Gunn, J.E., et al. 1998, AJ, 116, 3040

Harris, H.C., et al. 2003, AJ, submitted

Hogg, D.W., Finkbeiner, D.P., Schlegel, D.J., & Gunn, J.E. 2001, AJ, 122, 2129

Kawka, A., Vennes, S., Schmidt, G.D., Wickramasinghe, D.T., & Koch, R. 2003, MNRAS, in preparation

Kemic, S.B. 1975, Ap&SS, 36, 459

Kemic, S.B. 1974, JILA Rep. 113, Univ. of Colorado

Liebert, J., Angel, J.R.P., Stockman, H.S., & Beaver, E.A. 1978, ApJ, 225, 181

Latter, W.B., Schmidt, G.D., & Green, R.F. 1987, ApJ, 320, 308

Liebert, J. 1977, PASP, 89, 78

________. 1983, ApJ, 95, 878

________.1988, PASP, 100, 1302

Liebert, J., Bergeron, P., & Holberg, J.B. 2003, AJ, 125, 348

Liebert, J., Bergeron, P., Schmidt, G.D., & Saffer, R.A. 1993, ApJ, 418, 426

Lupton, R.H., Gunn, J.E., & Szalay, A. 1999, AJ, 118, 1406

Lupton, R.H., Gunn, J.E., Ivezic, Z., Knapp, G.R., Kent, S.M., & Yasuda, N. 2002, ASP Conf. Ser. 238, p. 269

Mathys, G. 2001, in ASP Conf. Ser. 248, Magnetic Fields Across the Hertzsprung-Russell Diagram, ed. G. Mathys, S.K. Solanki, & D.T. Wickramasinghe (San Francisco: ASP), 267

Muslimov, A.G., Van Horn, H.M., & Wood, M.A. 1995, ApJ, 442, 758

Pelletier, C., Fontaine, G., Wesemael, F., Michaud, G., & Wegner, G. 1986, ApJ, 307, 242

Pier, J.R., Munn, J.A., Hindsley, R.B., Hennessy, G.S., Kent, S.M., Lupton, R.H., & Ivezic, Z. 2003, AJ, 125, 1559

Reid, I.N., Liebert, J., & Schmidt, G.D. 2001, ApJ, 550, L61

Reimers, D., Jordan, S., Beckman, V., Christlieb, N., & Wisotzki, L. 1998, A&A, 337, L13

Ruder, H. Wunner, G., Herold, H., & Geyer, F. 1994, Atoms in Strong Magnetic Fields (Berlin: Springer)

Schmidt, G.D. 1989, in White Dwarfs, Proc. IAU Colloquium 114, G. Wegner, ed. (Berlin: Springer-Verlag), 305

Schmidt, G.D., Bergeron, P., Liebert, J., & Saffer, R.A. 1992, ApJ, 394, 603

Schmidt, G.D., Liebert, J., Harris, H.C., Dahn, C.C., & Leggett, S.K. 1999, ApJ, 512, 916

Schmidt, G.D., & Smith, P.S. 1995, ApJ, 448, 305

Schmidt, G.D., Stockman, H.S., & Smith, P.S. 1992, ApJ, 398, L57

Schmidt, G.D., Vennes, S., Wickramasinghe, D.T., & Ferrario, L. 2001, MNRAS, 328, 203

Sion, E.M., Fritz, M.L., McMullin, J.P., & Lallo, M.D. 1988, AJ, 96, 251

Smith, J.A., et al 2002, AJ, 123, 2121

Stoughton, C. et al. 2002, AJ, 123, 485

Vennes, S., Schmidt, G.D., Ferrario, L., Christian, D.J., Wickramasinghe, D.T., & Kawka, A. 2003, ApJ, in press

Wickramasinghe, D.T., & Ferrario, L. 2000, PASP, 112, 873

York, D.G. et al. 2000, AJ, 120, 1579

Table 1
SDSS DA MAGNETIC WHITE DWARFS

Star (SDSS+)	Pl.-MJD-Fib.	UT Date	UT	B_p (MG)	i (°)	Comment
J004248.19+001955.3	690-52261-594	2001-12-18	3:12	14	30	DAH+DA pair; not in DR1
J021116.34+003128.5	405-51816-382	2000-09-29	9:58	490	···	
J030407.40−002541.7	411-51817-172	2000-09-30	10:37	11	60	(1: 10.8 MG, 50°)
J033145.69+004517.0	415-51810-370	2000-09-23	8:34	12	60	KUV03292+0035; (1: 12.1 MG, 55°)
J034308.18−064127.3	462-51909-117	2000-12-31	5:16	13	45	
J034511.11+003444.3	416-51811-590	2000-09-24	9:35	1.5	0	(1: 1.5 MG, 0°)
J075819.57+354443.7	757-52238-144	2001-11-25	8:12	27	30	
J075959.56+433521.3	437-51869-369	2000-11-21	10:18	220	···	G111-49
J080743.33+393829.2	545-52202-009	2001-10-20	11:00	49	30	
J084155.74+022350.6	564-52224-248	2001-11-08	11:09	6	90	
J084716.21+484220.4	550-51959-629	2001-02-19	4:40	∼3	···	DAH+DB pair
J085830.85+412635.1	830-52293-070	2002-01-19	5:44	2	30	not in DR1
J092527.47+011328.7	475-51965-315	2001-02-25	7:53	2.2	···	
J100005.67+015859.2	500-51994-557	2001-03-26	2:47	20	30	
J101618.37+040920.6	574-52355-166	2002-03-21	4:09	7.5	30	not in DR1
J101805.04+011123.5	503-51999-244	2001-03-26	4:19	120	···	PG1015+015
J105404.38+593333.3	561-52295-008	2002-01-21	9:05	17	90	not in DR1
J105628.49+652313.5	490-51929-205	2001-01-15	9:17	28	60	
J111010.50+600141.4	950-52378-568	2002-04-14	7:56	6.5	70	not in DR1
J112852.88−010540.8	326-52375-565	2002-04-11	4:41	3	60	not in DR1
J113357.66+515204.8	879-52365-586	2002-04-01	7:11	7.5	90	not in DR1
J113839.51−014903.0	327-52294-583	2002-01-12	10:29	24	60	LBQS1136−0132; not in DR1
J114006.37+611008.2	776-52319-042	2002-02-14	9:29	58	20	not in DR1
J115418.14+011711.4	515-52051-126	2001-05-20	4:22	32	45	
J115917.39+613914.3	777-52320-069	2002-02-15	9:41	15.5	60	not in DR1
J121209.31+013627.7	518-52282-285	2002-01-08	12:01	13	80	not in DR1
J121635.37−002656.2	288-52000-276	2001-04-01	6:24	61	90	(1: 63 MG, 75°)
J122209.44+001534.0	289-51990-349	2001-03-22	6:25	14	80	(1: 12 MG, 40°)
J124851.31−022924.7	337-51997-264	2001-03-29	7:36	7	40	
J133340.34+640627.4	603-52056-112	2001-05-27	5:20	13	60	
J134043.10+654349.2	497-51989-182	2001-03-21	9:14	3	60	
J144614.00+590216.7	608-52081-140	2001-06-21	4:03	7	70	
J151745.19+610543.6	613-52345-446	2002-03-09	12:19	17	30	not in DR1
J153532.25+421305.6	1052-52466-252	2002-07-10	5:04	4.5	60	not in DR1
J153829.29+530604.6	795-52378-637	2002-04-14	10:27	12	30	not in DR1
J154213.48+034800.4	594-52045-400	2001-05-16	8:47	8	60	
J160437.36+490809.2	622-52054-330	2001-05-25	8:48	53	0	
J165203.68+352815.8	820-52438-299	2002-06-13	8:14	9.5	60	not in DR1
J172045.37+561214.9	367-51997-461	2001-03-22	11:51	21	30	(1: 21 MG, 85°)
J172329.14+540755.8	359-51821-415	2000-10-03	4:00	35	10	(1: 33 MG, 35°)
J172932.48+563204.1	358-51818-239	2000-10-01	2:16	28	···	
J204626.15−071037.0	635-52145-227	2001-08-24	4:40	2	60	
J205233.52−001610.7	982-52466-019	2002-07-11	7:08	13	80	not in DR1
J214930.74−072812.0	644-52173-350	2001-09-21	4:37	42	30	
J215135.00+003140.5	371-52078-500	2001-06-12	9:37	∼300	···	
J215148.31+125525.5	733-52207-522	2001-10-25	4:21	21	90	not in DR1
J221828.59−000012.2	374-51791-583	2000-09-04	5:19	225	30	
J224741.46+145638.8	740-52263-444	2001-12-20	2:50	560	···	not in DR1
J232248.22+003900.9	383-51818-421	2000-10-01	4:29	19	60	(1: 13 MG, 25°)

References. — (1) Gänsicke et al. (2002)

Table 2

SDSS DB MAGNETIC WHITE DWARFS

Star (SDSS+)	Pl.-MJD-Fib.	UT Date	UT	B_p (MG)	i (°)	Comment
J001742.44+004137.4	687-52518-510	2002-09-01	9:44	8.3	90	not in DR1
J014245.37+131546.4	429-51820-311	2000-10-01	6:18	4	60	
J232337.55−004628.2	383-51818-215	2000-10-01	4:29	4.8	30	(1)

References. — (1) Gänsicke et al. (2002)

Table 3

ADDITIONAL SDSS MAGNETIC WHITE DWARFS

Star (SDSS+)	Pl.-MJD-Fib.	UT Date	UT	B_s (MG)	Comment
J000555.91−100213.4	650-52143-037	2001-08-22	7:37	?	DQ?
J015748.15+003315.1	700-52199-627	2001-10-16	8:30	3.7	DZ; not in DR1
J033320.37+000720.7	415-51810-492	2000-09-23	8:34	?	HE0330−0002; (1)
J093313.14+005135.4	475-51965-003	2001-02-25	7:53	?	resembles LHS2229
J103655.38+652252.0	489-51930-520	2001-01-21	9:17	4:	DQ; (2)
J111341.33+014641.7	510-52381-184	2002-04-17	4:20	?	resembles LP790-29; not in DR1
J121456.39−023402.8	333-52313-399	2002-02-07	11:54	1.9	DZ; LHS 2534; not in DR1
J133359.86+001654.8	298-51662-484	2000-04-28	5:47	?	resembles LHS2229

References. — (1) Gänsicke et al. (2002); (2) Liebert et al. (2003)

Table 4
PHOTOMETRY OF SDSS MAGNETIC WHITE DWARFS

Star (SDSS+)	u	g	r	i	z	$T_{\rm eff}$ (K)
J000555.91−100213.4	17.31	17.69	18.11	18.46	18.76	···
J001742.44+004137.4	16.86	16.96	17.21	17.44	17.71	15,000
J004248.19+001955.3	19.79	19.48	19.58	19.68	19.73	11,000
J014245.37+131546.4	17.61	17.69	17.99	18.20	18.44	15,000
J015748.15+003315.1	21.22	19.53	19.20	19.23	19.32	···
J021116.34+003128.5	18.66	18.55	18.52	18.63	18.73	9,000:
J030407.40−002541.7	18.06	17.80	17.93	18.11	18.35	11,500
J033145.69+004517.0	17.31	17.22	17.47	17.72	18.00	15,500
J033320.37+000720.7	17.03	16.56	16.43	16.42	16.52	7,500:
J034308.18−064127.3	19.49	19.47	19.60	19.81	19.92	13,000:
J034511.11+003444.3	19.18	18.66	18.53	18.50	18.52	7,500
J075819.57+354443.7	18.07	18.18	18.56	18.83	19.01	22,000
J075959.56+433521.3	16.76	16.19	16.23	16.21	16.09	9,000:
J080743.33+393829.2	20.41	20.14	20.33	20.57	20.60	13,000
J084155.74+022350.6	19.57	18.99	18.80	18.72	18.77	7,000
J084716.21+484220.4	17.86	17.88	18.20	18.48	18.68	19,000
J085830.85+412635.1	17.73	17.05	16.89	16.83	16.88	7,000:
J092527.47+011328.7	19.04	18.59	18.69	18.76	18.86	10,000
J093313.14+005135.4	19.80	19.59	19.28	19.33	19.45	···
J100005.67+015859.2	20.39	20.03	20.04	20.06	20.28	9,000
J101618.37+040920.6	20.56	20.30	20.36	20.49	20.33	10,000
J101805.04+011123.5	16.52	16.28	16.44	16.55	16.74	12,500:
J103655.38+652252.0	18.31	18.52	18.85	19.15	19.26	···
J105404.38+593333.3	20.58	20.23	20.28	20.45	20.40	9,500
J105628.49+652313.5	19.83	19.70	19.99	20.31	20.49	16,500
J111010.50+600141.4	17.68	17.96	18.43	18.73	19.04	30,000
J111341.33+014641.7	18.62	19.21	18.47	18.26	18.10	···
J112852.88−010540.8	20.66	20.41	20.51	20.77	20.61	11,000
J113357.66+515204.8	17.26	17.34	17.71	18.01	18.33	22,000
J113839.51−014903.0	17.97	17.62	17.73	17.95	18.18	10,500
J114006.37+611008.2	20.02	19.64	19.90	20.06	20.20	13,500
J115418.14+011711.4	17.46	17.75	18.15	18.45	18.80	27,000:
J115917.39+613914.3	18.87	18.96	19.39	19.66	19.85	23,000
J121209.31+013627.7	18.43	17.99	18.07	18.24	18.40	10,000
J121456.39−023402.8	20.90	18.31	17.74	17.55	17.50	···
J121635.37−002656.2	19.86	19.60	19.87	20.09	20.11	15,000
J122209.44+001534.0	20.56	20.27	20.50	20.67	21.21	14,000
J124851.31−022924.7	18.71	18.38	18.62	18.87	19.19	13,500
J133340.34+640627.4	18.16	17.88	18.10	18.25	18.56	13,500
J133359.86+001654.8	19.06	19.41	18.33	18.06	18.16	···
J134043.10+654349.2	18.74	18.42	18.74	18.95	19.23	15,000
J144614.00+590216.7	20.55	20.10	20.31	20.44	20.59	12,500
J151745.19+610543.6	20.85	20.50	20.55	20.74	21.17	9,500
J153532.25+421305.6	20.46	20.36	20.74	20.89	22.04	18,500
J153829.29+530604.6	19.53	19.29	19.49	19.67	20.03	13,500
J154213.48+034800.4	19.56	19.11	19.11	19.22	19.43	8,500
J160437.36+490809.2	18.22	17.90	17.91	18.00	18.15	9,000
J165203.68+352815.8	19.68	19.25	19.42	19.54	19.75	11,500
J172045.37+561214.9	19.99	20.10	20.47	20.72	21.30	22,000
J172329.14+540755.8	19.10	18.78	18.85	19.01	19.27	10,000
J172932.48+563204.1	20.24	20.02	20.08	20.21	20.87	10,500
J204626.15−071037.0	18.32	17.99	17.90	17.95	18.02	8,000
J205233.52−001610.7	18.44	18.50	18.80	19.09	19.44	19,000

Table 4—*Continued*

Star (SDSS+)	u	g	r	i	z	$T_{\rm eff}$ (K)
J214930.74−072812.0	17.36	17.43	17.80	18.12	18.36	22,000:
J215135.00+003140.5	18.16	17.84	17.84	17.87	18.03	9,000:
J215148.31+125525.5	18.30	18.11	18.32	18.58	18.80	14,000
J221828.59−000012.2	18.29	18.06	18.35	18.54	18.71	15,500:
J224741.46+145638.8	17.31	17.38	17.62	17.95	18.20	18,000:
J232248.22+003900.9	18.96	19.22	19.43	19.69	19.85	20,000:
J232337.55−004628.2	17.88	18.02	18.31	18.54	18.77	15,000

Table 5

UNRECOVERED MAGNETIC WHITE DWARFS IN IMAGED AREAS[a]

Star	SDSS Coordinates (J2000) (*hh*:*mm*:*ss.ss* ±*dd*:*mm*:*ss.s*)	u	g	r	i	z
Feige 7	00:43:45.98 −10:00:25.1	14.25	14.40	14.75	15.02	15.32
G99-37	05:51:19.49 −00:10:20.6	15.37	14.72	14.39	14.32	14.38
GD90	08:19:46.35 +37:31:27.7	16.10	15.73	15.85	16.02	16.28
G195-19	09:15:55.97 +53:25:23.0	14.49	13.99:	14.08:	13.84:	13.98

[a] All but GD90 exceed the brightness threshold for being assigned a spectroscopic fiber.

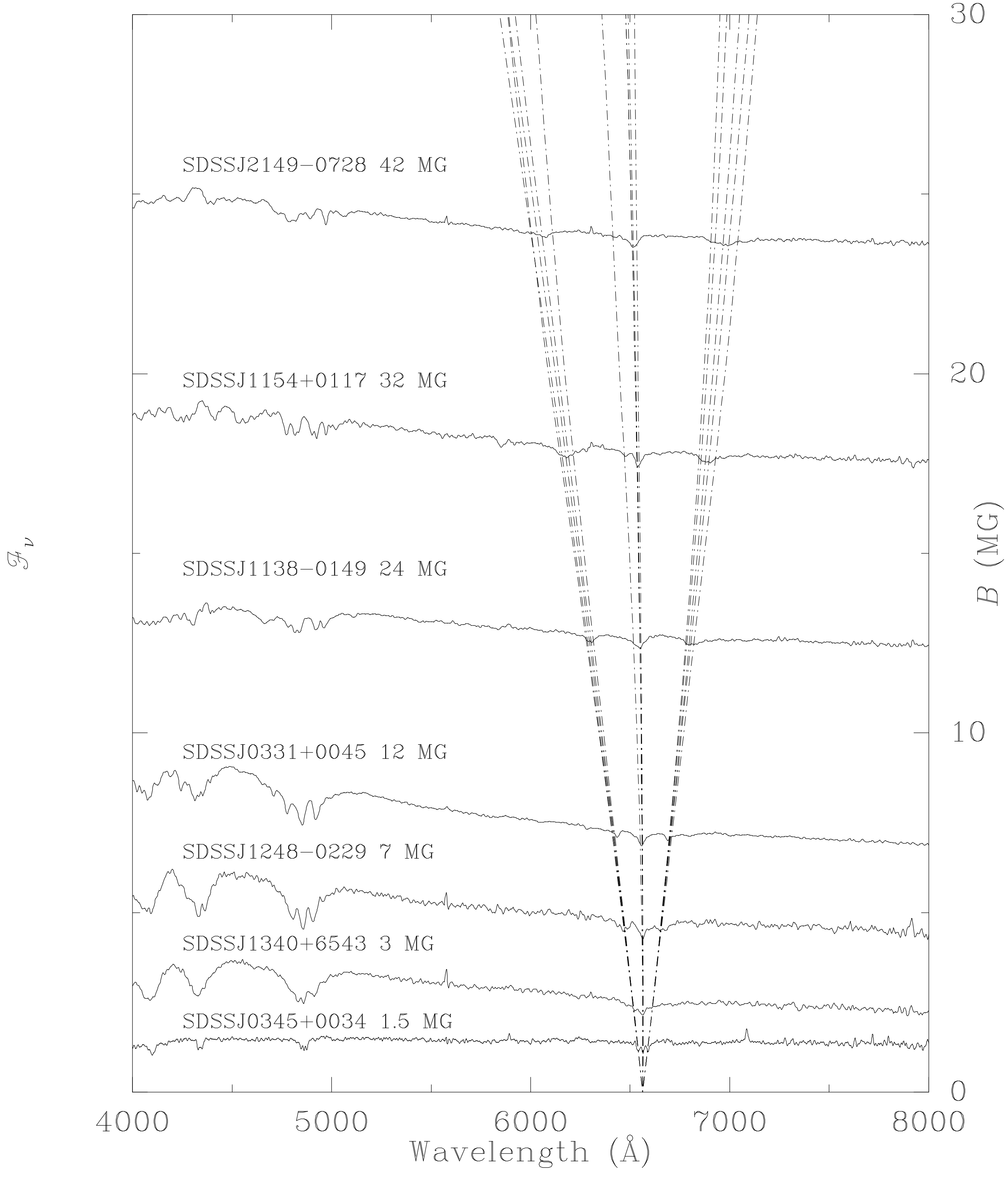

FIG. 1.— A sample of the DR1 magnetic DA white dwarfs showing polar fields from 1.5 MG to 42 MG as indicated. For brevity, stars are indicated by SDSS J*hhmm*±*ddmm*. Spectra are positioned along the ordinate according to approximate mean surface field strength, B_s, in order to match absorption features with the locations of Zeeman components of Hα for $0 < B < 30$ MG.

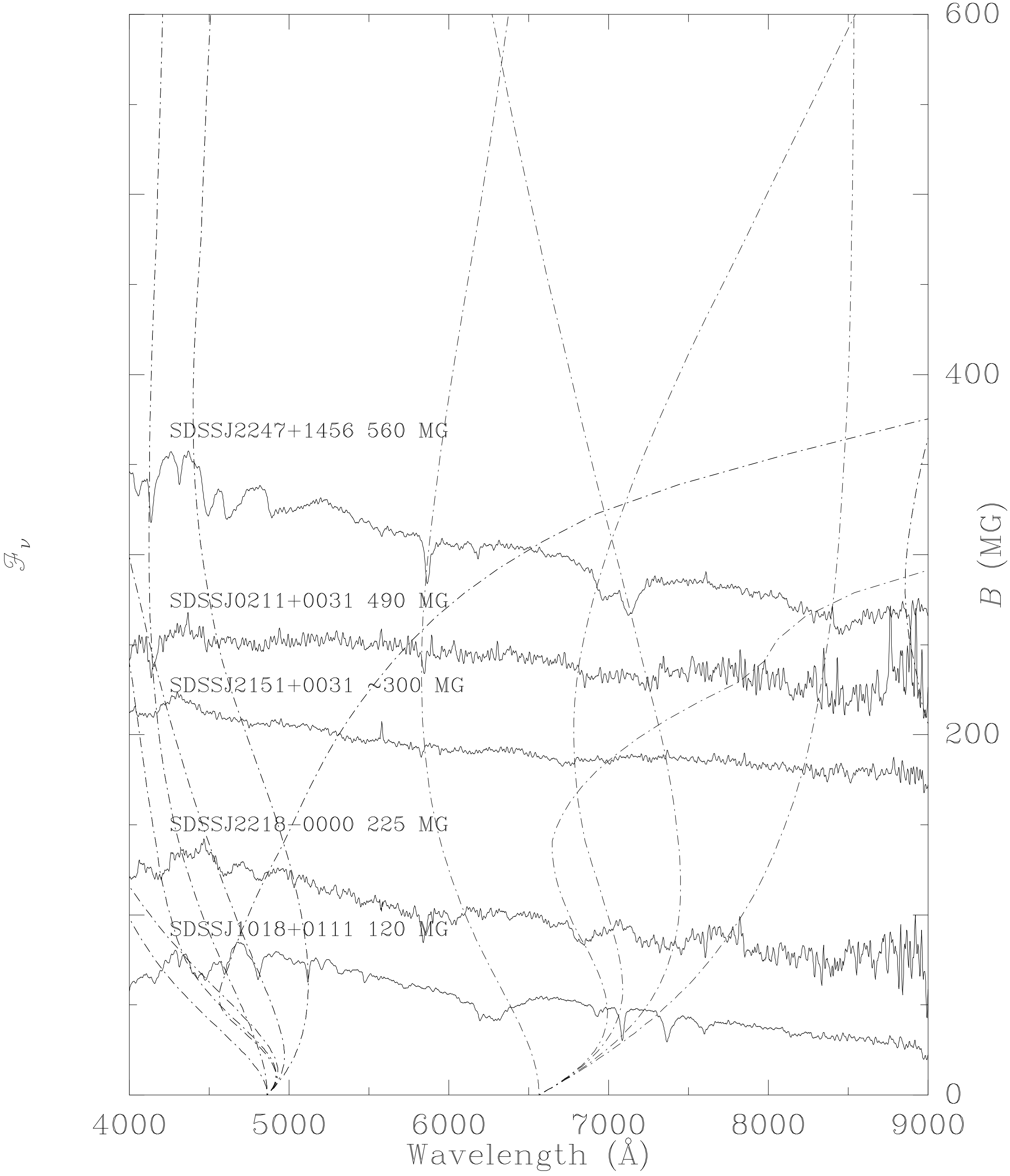

FIG. 2.— Magnetic DA white dwarfs from the DR1 with polar field strengths $B_p = 100$ MG $-$ 500 MG compared to those components of the Balmer series that undergo turnarounds or reach stationary points in the region of interest. Spectra are positioned along the ordinate by the approximate mean surface field strength B_s.

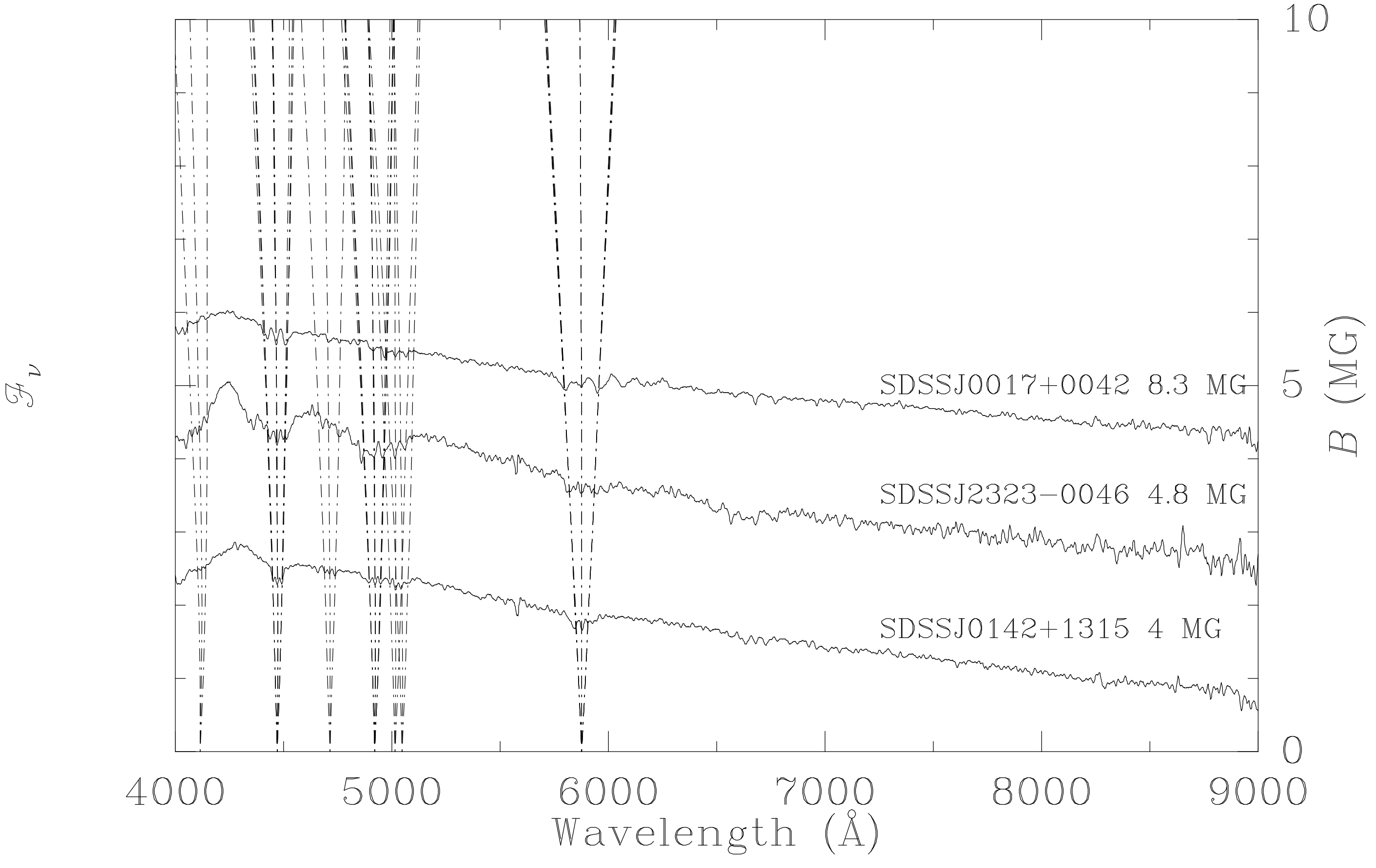

FIG. 3.— As in Figures 1 and 2 for magnetic DB white dwarfs with $B_p < 10$ MG. The behavior of several He I lines is also shown for comparison.

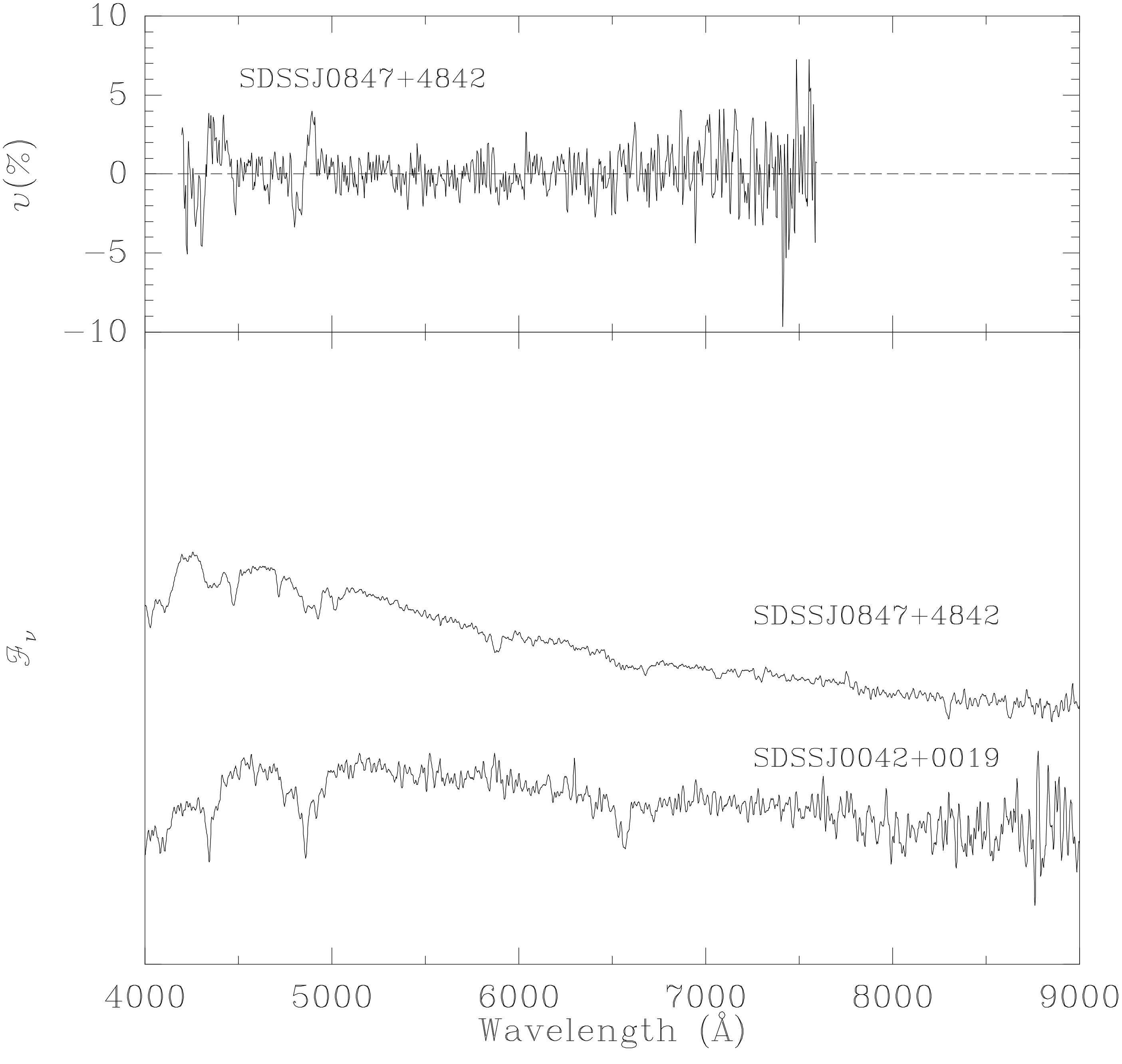

FIG. 4.— New magnetic + nonmagnetic white dwarf binaries. *(Bottom):* The DAH+DA pair SDSS J0042+0019 with $B_p = 14$ MG and the apparent DAH+DB SDSS J0847+4842 with $B_p \sim 3$ MG. Note the breadth of, e.g., Hα vs. the He I lines in the latter star. *(Top):* Circular spectropolarimetry of SDSS J0847+4842 showing polarization reversals across Hβ and Hγ, but not across the He I lines.

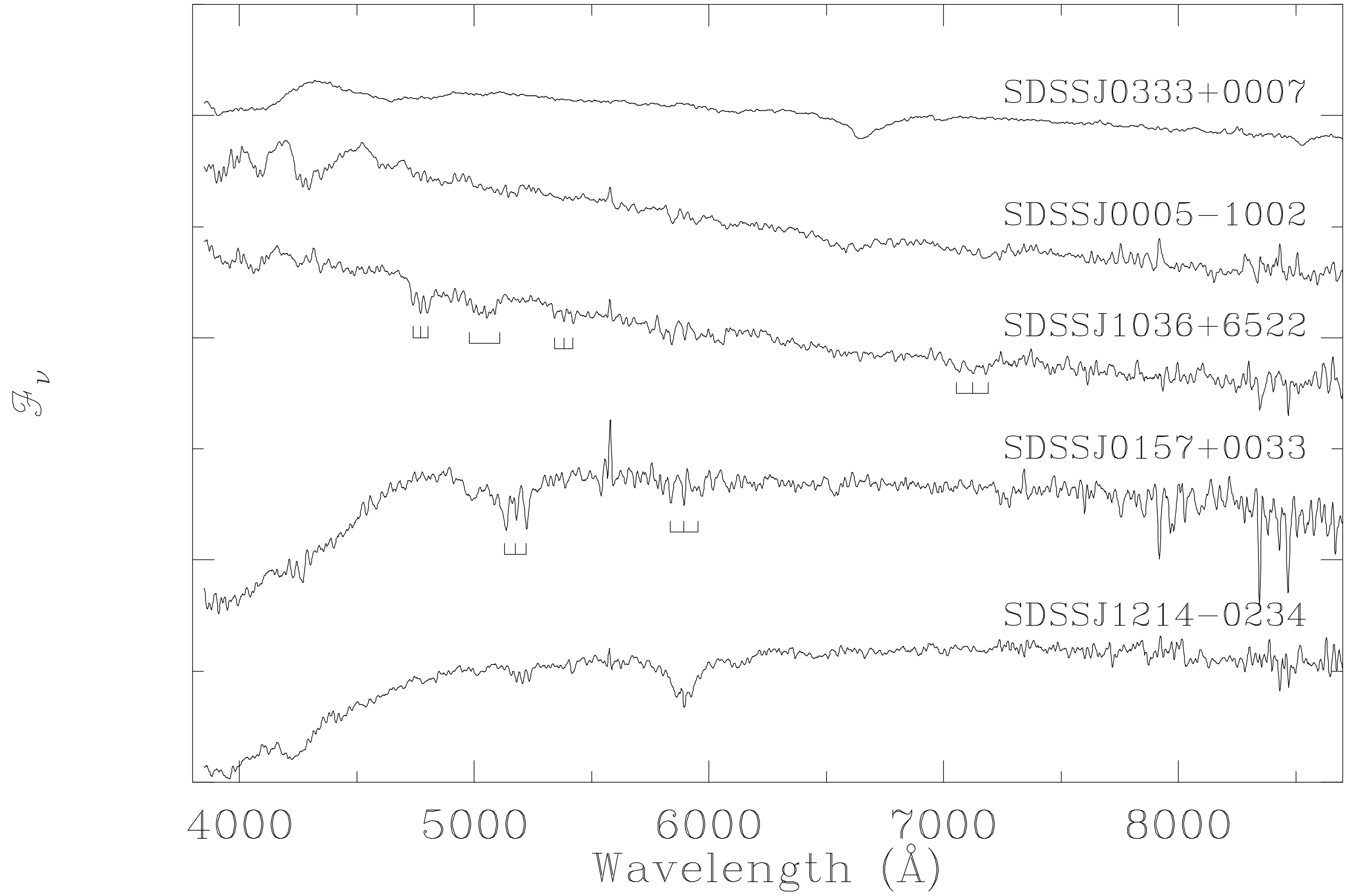

FIG. 5.— SDSS spectra of magnetic white dwarfs and white dwarf candidates of various types. SDSS J1214−0234 (=LHS 2534) and SDSS J0157+0033 are magnetic DZ stars showing Zeeman-split lines of Na I and Mg I at $B_s = 1.9$ and 3.7 MG, respectively. SDSS J1036+6522 is the first magnetic DQ star to show split C I lines. SDSS J0005−1002 may be similar in nature, but requires confirmation. Spectropolarimetry of SDSS J0333+0007 (=HE0330−0002) proves it to be magnetic, but the distorted features do not correspond with a known atomic or molecular species. Data artifacts affect the spectra of the faintest stars for $\lambda \gtrsim 8000$ Å.

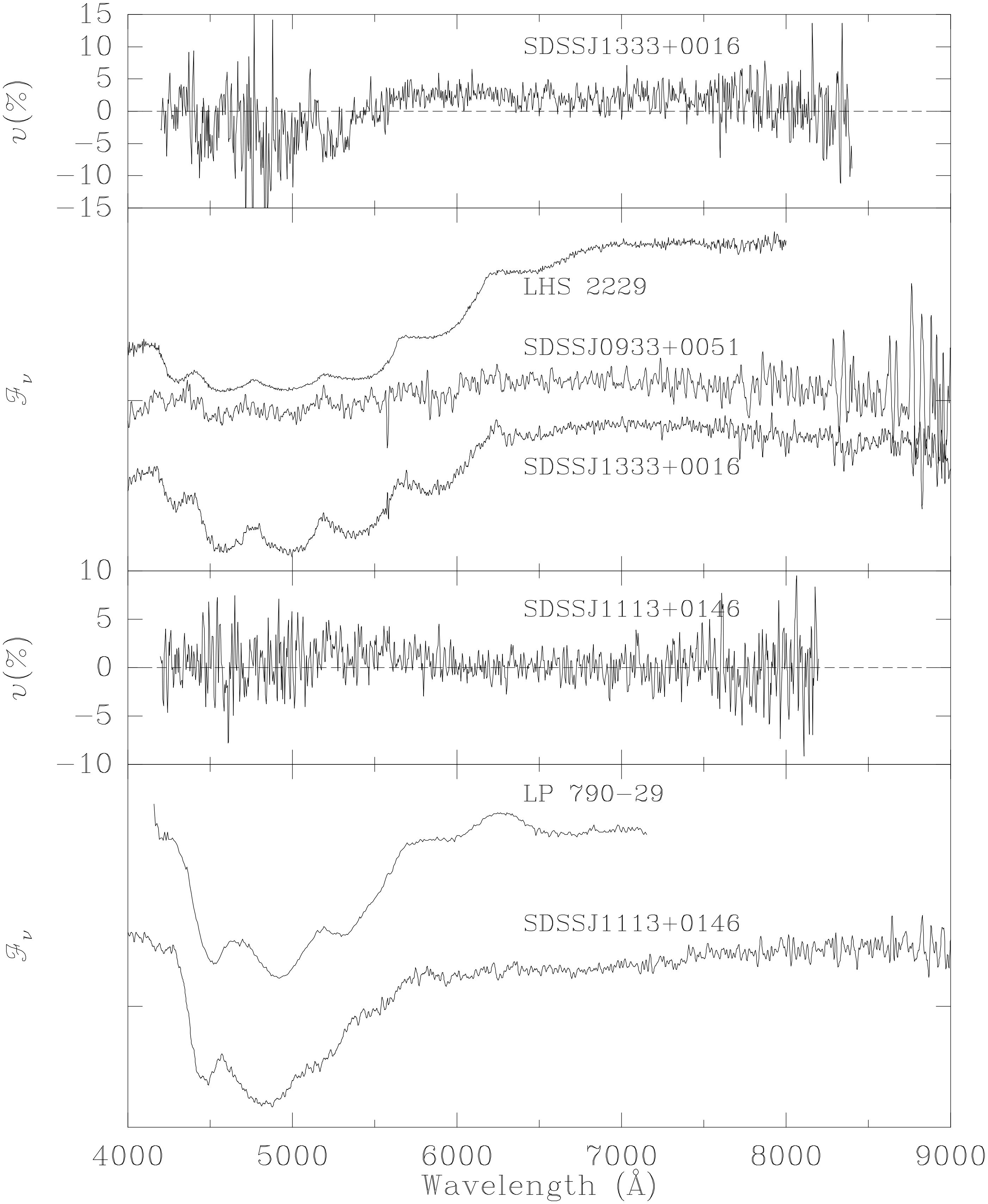

FIG. 6.— New SDSS white dwarfs showing molecular features compared to previously-known examples with very similar spectra. The spectra of LHS 2229 and LP 790-29 have been displaced upward for clarity. Spectropolarimetry demonstrates that SDSS J1113+146 and SDSS J1333+0016 are magnetic, with the features in SDSS J1113+0146 and LP 790-29 likely being the C_2 Swan bands. The species responsible for the remarkable series in SDSS J1333+0016 and LHS 2229 are not yet known. SDSS J0933+0051 appears to exhibit the same band structure, but the features are much weaker.

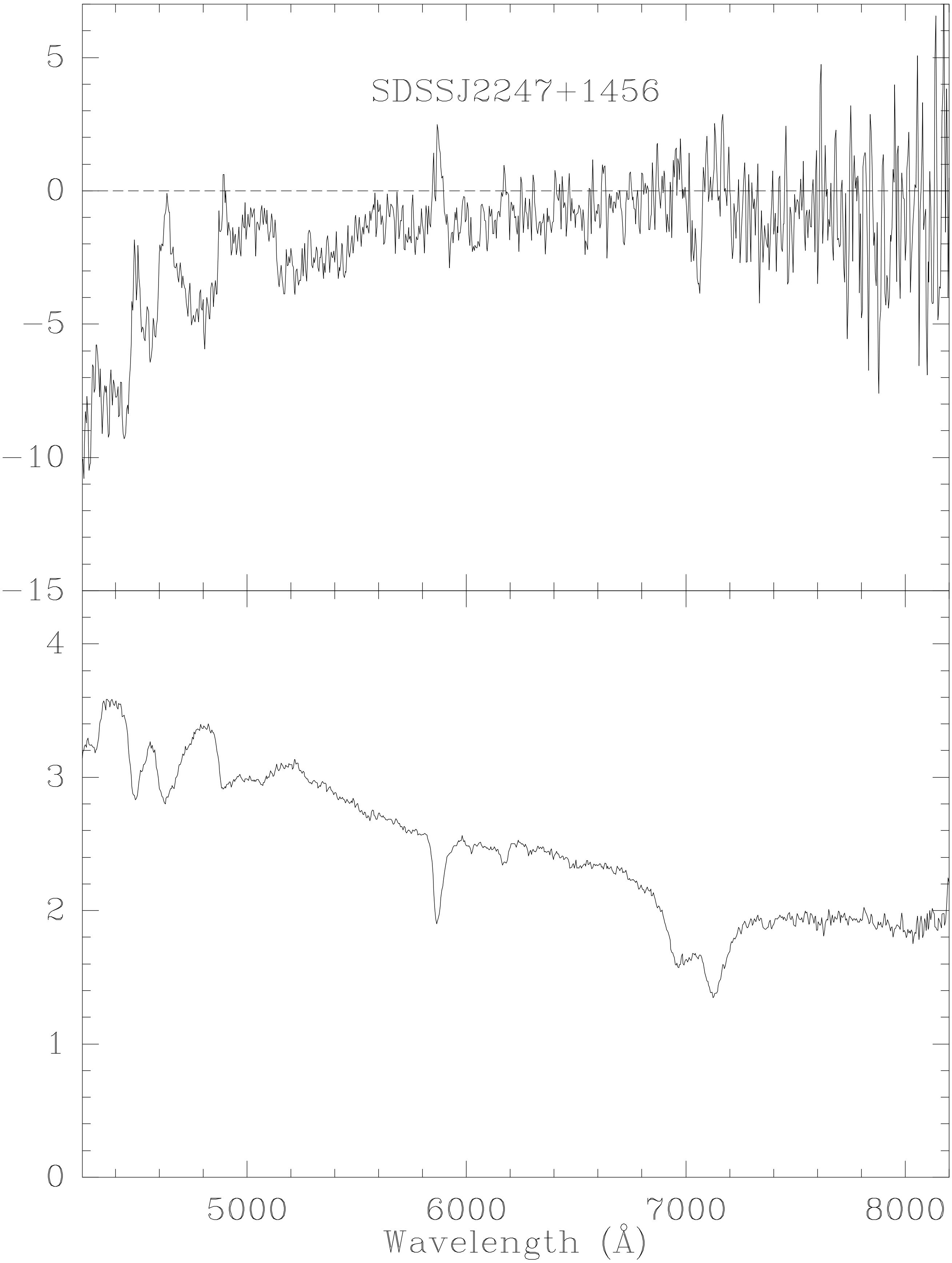

FIG. 7.— Circular polarization *(top)* and total flux *(bottom)* spectra of a new hydrogen-atmosphere SDSS magnetic white dwarf with $B_p \sim 560$ MG.

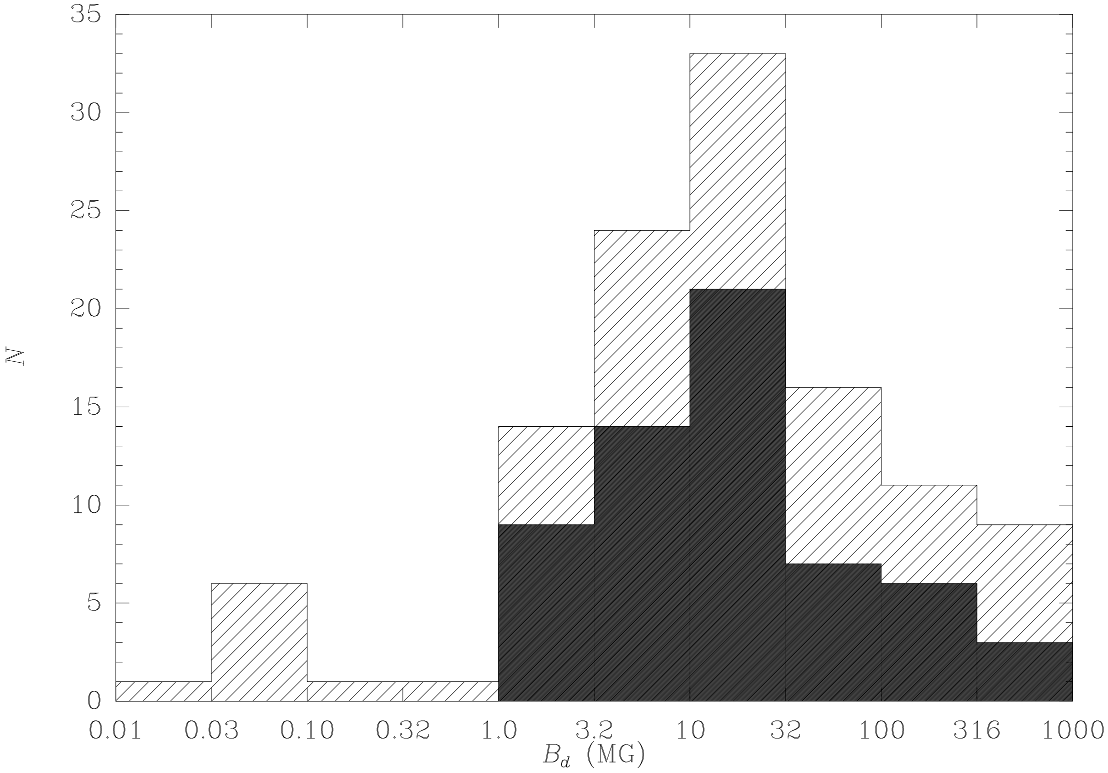

FIG. 8.— Histogram of magnetic white dwarfs in equal intervals of $\log B$. SDSS discoveries are shaded black; the distribution for all known magnetic white dwarfs is hatched. Selection effects are not likely to affect the overall distribution of stars with $B_p \gtrsim 3$ MG, so the general peak in the range $\sim 5-30$ MG is considered to be real.